

Lateral tunneling in point contacts

T. Bever, A. D. Wieck, K. v. Klitzing, and K. Ploog
*Max-Planck-Institut für Festkörperforschung, Heisenbergstrasse 1,
 D-7000 Stuttgart 80, Federal Republic of Germany*

(Received 25 February 1991)

The Shubnikov-de Haas oscillations of the resistance of a point contact formed in the two-dimensional electron gas of $\text{Al}_x\text{Ga}_{1-x}\text{As}/\text{GaAs}$ heterostructures via the lateral field effect are investigated for a series of values of the confining gate voltage V_g . Giant magnetoresistance oscillations are observed for values of V_g close to the threshold voltage. An analysis of the differential channel resistance dV/dI as a function of the voltage drop V over the point contact shows that these oscillations are due to lateral tunneling through the point contact.

Quasi-one-dimensional (1D) quantum point contacts have attracted considerable interest since the discovery of quantized conductance in multiples of $2e^2/h$.^{1,2} These systems were induced via split gates on top of $\text{Al}_x\text{Ga}_{1-x}\text{As}/\text{GaAs}$ heterostructures containing a high-mobility two-dimensional electron gas (2DEG). More recently, in-plane-gated (IPG) quantum wires have been fabricated by means of focused ion-beam (FIB) insulation writing, which also show the conductance quantization.³ These devices have turned out to be rugged enough to study higher voltage effects such as point contact spectroscopy.⁴ In this paper we present data from transport experiments on a FIB written point contact. We show that the width of the quasi-1D channel can be tuned down to zero via the gate voltage V_g . In this limit transport between the 2DEG's adjacent to the channel occurs by lateral tunneling through a potential barrier in the channel. Previously reported experiments on lateral tunneling were done on electric-field induced depletion barriers via 50–60-nm thin metal stripes evaporated on top of $\text{Al}_x\text{Ga}_{1-x}\text{As}/\text{GaAs}$ heterostructures with a lateral width (perpendicular to the current direction) of more than $0.5 \mu\text{m}$.^{5–7} In our device the electrons tunnel through a tunable potential barrier induced by the in-plane electric field and they are, therefore, laterally restricted to the dimensions of the point contact. There have been a number of experiments^{8–11} and theoretical considerations¹² concerning the quantum Hall effect in quasi-1D systems. Here we report giant magnetoresistance oscillations in the tunneling regime.

All samples discussed in the following are prepared from $\text{GaAs}/\text{Al}_{0.3}\text{Ga}_{0.7}\text{As}$ heterostructures grown by molecular-beam epitaxy with carrier densities $n = 2.1 \times 10^{11}$, 2.9×10^{11} , and $4.6 \times 10^{11} \text{ cm}^{-2}$, and zero-field mobilities of $\mu = 3.0 \times 10^5$, 6.5×10^5 , and $6.0 \times 10^5 \text{ cm}^2/\text{Vs}$ at $T = 4 \text{ K}$ for samples *A*, *B*, and *C*, respectively. The as-grown samples are mesa etched with standard optical lithography to define a $150\text{-}\mu\text{m}$ wide Hall bar with $150 \mu\text{m}$ spaced $50\text{-}\mu\text{m}$ wide potential probes. By means of focused 100-keV Ga^+ -ion-beam insulation writing with a spot diameter of 100 nm and a dose of $1 \times 10^{13} \text{ cm}^{-2}$ we create an IPG.³ In combination with an insulating line written from the sample edge close to the gate, this gives a tunable constriction (see inset of Fig. 1). We denote the shortest dis-

tance across the constriction between the center points of the FIB-exposed spots as the geometrical width, w_{geo} ($w_{\text{geo}} = 2, 2, \text{ and } 1.5 \mu\text{m}$ for samples *A*, *B*, and *C*, respectively). By applying a positive (negative) gate voltage to terminal 6 (see inset Fig. 1) with respect to the source, both the effective width and the carrier concentration of the constriction can be increased (decreased). The leakage current between gate and source (drain) is well below 100 pA for all samples in the gate voltage range used in the presented experiments. All measurements are performed in a bath cryostat at 1.6 K . The magnetoresistance is measured in a four contact configuration using the standard lock-in technique with a 10 nA ac current of frequency 86 Hz in magnetic fields up to 8 T . The dc drain-source bias V is obtained by superimposing on the ac current a constant dc current I through the device.

In Fig. 1 we show the typical dependence of the channel resistance R at zero bias on the applied gate voltage V_g . Subtracting an offset resistance R_0 of typically $2\text{--}3 \text{ k}\Omega$ which results from the large aspect ratio of the channel leads in the 2DEG, the channel conductance $G = 1/(R - R_0)$ shows an almost linear dependence on the gate

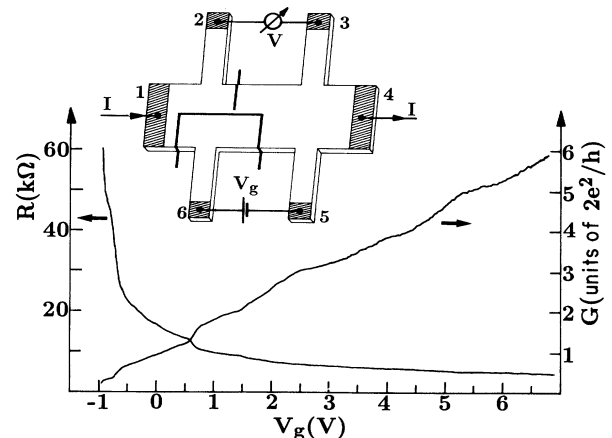


FIG. 1. Measured channel resistance R and conductance G [$G = (R - R_0)^{-1}$, $R_0 = 2.7 \text{ k}\Omega$] as a function of the applied gate voltage. The inset shows a sketch of the sample with the focused ion-beam written path indicated by the bold lines.

voltage. Steplike structures can be seen for values of G equal to multiples of $2e^2/h$ resulting from the well-known conductance quantization. Both effective width w and carrier concentration n of the channel are tuned down to zero as the gate voltage is decreased. We denote the gate voltage at which G extrapolates to zero the threshold voltage V_{th} .

Figure 2(a) shows the differential channel resistance dV/dI as a function of the source-drain voltage for different values of V_g . When V_g is close to V_{th} [uppermost curve in Fig. 2(a)] the differential resistance dV/dI has a maximum around zero bias and decreases drastically as the bias V is increased to 4 mV. This non-Ohmic behavior can be explained by the following model. Assuming ballistic transport, the net current I in a single 1D subband (at zero temperature) is given by

$$I = e \int_{E_F - eV/2}^{E_F + eV/2} v(E) N(E) T(E) dE, \quad (1)$$

where v is the drift velocity, N the 1D electronic density of states, T the transmission probability, and E_F the Fermi energy of the system. Since in the 1D case the product $v(E)N(E)$ is energy independent, Eq. (1) reduces to

$$I = 2e/h \int_{E_F - eV/2}^{E_F + eV/2} T(E) dE. \quad (2)$$

If electrons are fully transmitted through the constriction [$T(E)=1$] and as long as 1D subbands are below E_F one gets the well-known conductance quantization from Eq. (2). This is the case as long as $R - R_0 \leq h/2e^2$. In Fig. 2(a) (uppermost curve), however, $R \gg h/2e^2$. In this limit the confining gate voltage causes a potential barrier in the channel and to get a current, electrons have to tunnel laterally through the barrier from one side to the other [see Fig. 2(b)]. We assume a barrier ϕ of parabolic shape $\phi(x) = \phi_0(1 - x^2/a^2)$ where x denotes the distance from the center of the constriction in the direction of the current. It should be pointed out that the electrons, when tunneling through the barrier, still feel the confining gate potential with an electric-field perpendicular to the

current flow in the plane of the 2DEG. The transmission probability is given by the well-known approximate expression¹³

$$T(E) = \exp \left[- \frac{4\pi\sqrt{2m}}{h} \int_{x_1}^{x_2} \sqrt{\psi(x) - E} dx \right] \quad (3)$$

with $m=0.07m_e$ (m_e free-electron mass) and for simplicity $\psi(x) = \phi(x) - eVx/2x_0$ for $-x_0 \leq x \leq x_0$, $\psi(x) = \phi(x) + eV/2$ for $x < -x_0$, and $\psi(x) = \phi(x) - eV/2$ for $x > x_0$ [x_0 as defined in Fig. 2(b)]. The integration limits x_1 and x_2 are the intersection points of the potential barrier ψ with E_F . The data from the uppermost curve in Fig. 2(a) can be fitted assuming a barrier height $\phi_0 - E_F = 3.3$ meV and a barrier length $2x_0 = 20$ nm [dotted line in Fig. 2(a)]. Even though the model is simplified, the values obtained from this fit are of the correct order of magnitude because the zero-bias resistance drops to half of its value at roughly 4 mV which should reflect the barrier height. Note that beyond $V \approx 4$ mV the differential resistance is determined by other processes.⁴ It should be pointed out that both barrier height and length can be tuned continuously by changing the gate voltage. The internal field in the tunnel junction is typically 2 mV/20 nm = 10^3 V/cm. It is much smaller than the electric field responsible for the 2D confinement ($\approx 10^4$ V/cm). The in-plane electric-field induced by V_g is typically 1 V/1 $\mu\text{m} = 10^4$ V/cm due to a n - p - n junction with depletion lengths of less than 1 μm at the interfaces of the FIB paths.¹⁴ Thus, the applied source-drain bias of a few mV represents only a weak perturbation of the electrostatically defined 1D channel.

In Fig. 3 both the source-drain voltage dependence and the Shubnikov-de Haas (SdH) oscillation of the differential channel resistance of sample B for different values of V_g are presented in the same plot. The bottom magnetoresistance curve ($V_g = +7.0$ V) has a broad zero resistance minimum at filling factor $i=2$ (6 T) and is perfectly periodic in $1/B$ with a carrier density which is the same as in the 2DEG ($n = 2.9 \times 10^{11}$ cm⁻²). Applying gate voltages $V_g < 7.0$ V the position of the minima shift to lower fields and are no longer periodic in $1/B$. Increasing the confining gate potential (i.e., decreasing V_g), both the 1D subbands and the Landau quantization determine the magnetotransport behavior of the device. The SdH-oscillation amplitude decreases and the channel resistance is nonzero at filling factor 2. This behavior changes drastically in the gate voltage regime where lateral tunneling takes place. Strong magnetoresistance oscillations appear with an amplitude much larger than the SdH-amplitude of the 2DEG adjacent to the channel. As indicated by the arrows in Fig. 3 the position of the minima of these oscillations is the same as for the SdH minima of the 2DEG. This is observed in all samples investigated. Figure 4 shows the magnetoresistance of sample C in the tunneling regime. The position of the minima in this curve correspond to the SdH minima of the 2DEG adjacent to the channel in sample C . As can be seen from the inset in Fig. 4 the background resistance increases roughly proportional to B^2 in the tunneling regime for $B > 2$ T. This has also been observed in the case of vertical tunneling structures.¹⁵ A simple explanation has been given by an in-

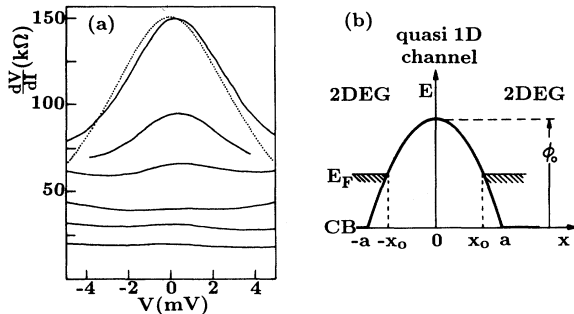


FIG. 2. (a) Measured differential channel resistance dV/dI of sample A as a function of the bias voltage V for gate voltages $V_g = 0.43, 0.22, -0.08, -0.28, -0.35,$ and -0.40 V for the lowest to the uppermost curve, respectively. The dotted curve is obtained from a fit as described in the text. (b) Potential barrier [conduction-band edge (CB)] as assumed for the model described in the text. The x coordinate denotes the direction of the current flow.

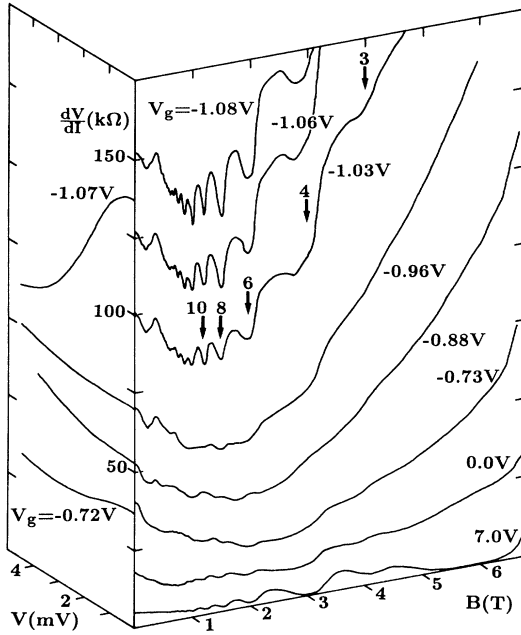


FIG. 3. Measured differential channel resistance of sample *B* for $B=0$ in the left-hand-side diagram for $V_g = -0.72, -0.88, -0.96,$ and -1.07 V for the lowest to the uppermost curves, respectively, and magnetoresistance of the same channel for $V=0$ in the right-hand-side diagram for $V_g = 7.0, 0.0, -0.73, -0.88, -0.96, -1.03, -1.06,$ and -1.08 V for the lowest to the uppermost curve, respectively. The arrows mark the position of the filling factors ($i=3-10$) of the 2DEG.

crease Δx of the effective tunneling path due to the sideways deflection of the ballistic electron by the magnetic field. Following Ref. 15, $\Delta x \approx aB^2$ where the constant a is a function of barrier height ϕ_0 and barrier length $2x_0$. Using typical values for ϕ_0 and $2x_0$ as given above and expanding the exponential function in Eq. (3), our data are nicely explained by this simple model for $B < 5$ T. Fertig and Halperin have given a detailed quantum-mechanical analysis of electrons in a magnetic field subjected to a quadratic saddle-point potential¹⁶ which is related to the potential discussed here. For increasing high magnetic field they obtain a decrease of the transmission probability T which is consistent with our data.

In order to explain the giant magnetoresistance oscillations we refer to a picture used in the literature¹⁷ which describes the screening behavior of electrons in the presence of an applied magnetic field. In the case of a half-filled Landau level (LL), screening should be optimum since the electrons are free to redistribute into many available states. The electrons are repelled by the field $d\phi/dx$ arising from the tunnel barrier in the constriction [see Fig. 2(b)]. For the point contact in the tunneling regime, this means that for a half-filled LL the barrier length $2x_0$ is enhanced. However, in the case of a filled LL the number of states at E_F is a minimum and the electrons cannot redistribute into more favorable states. For a filled LL the 2DEG is stiff and electrons are pushed closer towards the barrier. As a consequence the effective barrier length is

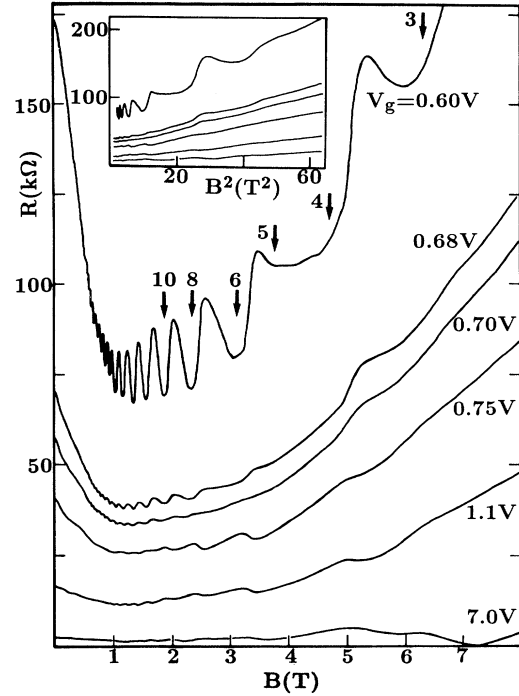


FIG. 4. Zero-bias magnetoresistance of the constriction in sample *C* for $V_g = 7.0, 1.1, 0.75, 0.70, 0.68,$ and 0.60 V for the lowest to the uppermost curves, respectively. The arrows mark the position of the filling factors ($i=3-10$) of the 2DEG. In the inset the curves for $V_g = 2.0, 1.1, 0.75, 0.70, 0.68,$ and 0.60 V are plotted vs B^2 . The labeling of the vertical axis of the inset refers to the lettering of the main figure.

decreased leading to higher tunneling probability and lower channel resistance. This explanation is consistent with our observation that minima in the tunneling resistance occur at integer filling factors. Note that other models based on the variation of E_F (and via E_F the effective barrier height $\phi_0 - E_F$) or the variation of the electronic density of states at the Fermi energy with magnetic field would lead to maxima instead of minima of the channel resistance at integer filling factors.

Finally, we would like to mention additional interesting features observed in our samples. All samples show a negative magnetoresistance in the tunneling regime which is most pronounced for sample *C* (uppermost curve in Fig. 4) resulting in a decrease of the channel resistance to half of its zero-field value at $B=1.2$ T. This effect can be explained as magnetic suppression of geometrical backscattering caused by the finite width of the point contact or backscattering caused by impurities in the channel.¹⁸ The amount of backscattering caused by the potential barrier in the point contact remains essentially unaffected by the low magnetic field. Sample *B* exhibits some structures in the magnetic-field range below 1 T. These structures appear when the zero-field resistance exceeds 50 k Ω and increase in strength as the gate voltage approaches V_{th} . Up to now we cannot give an explanation for this phenomenon.

In all samples the curves for those values of V_g at which

the zero-field resistance is approximately $50 \text{ k}\Omega$ give a rough border line beyond which lateral tunneling phenomena occur. This can be seen in Fig. 4. Maxima in the magnetoresistance curves for $V_g = 0.75 \text{ V}$ correspond to minima in the curve for $V_g = 0.68 \text{ V}$ whereas there is no more shift in the position of the minima for values of V_g even closer to V_{th} .

In conclusion we present in this paper data on lateral tunneling phenomena of quasi-1D channels in an applied magnetic field. Giant magnetoresistance oscillations are

observed, which we interpret as a consequence of the movement of the electrons in the 2DEG back and forth towards the point contact thereby changing the effective barrier length.

We would like to thank A. Fischer, M. Hauser, and R. Nötzel for their expert help in MBE growth, and U. Wulf for valuable discussions. We gratefully acknowledge financial support of the Bundesministerium für Forschung und Technologie of the Federal Republic of Germany.

-
- ¹B. J. van Wees, H. van Houten, C. W. J. Beenakker, J. G. Williamson, L. P. Kouwenhoven, D. van der Marel, and C. T. Foxon, *Phys. Rev. Lett.* **60**, 848 (1988).
- ²D. A. Wharam, T. J. Thornton, R. Newbury, M. Pepper, H. Ahmed, J. E. F. Frost, D. G. Hasko, D. C. Peacock, D. C. Ritchie, and G. A. C. Jones, *J. Phys. C* **21**, L209 (1988).
- ³A. D. Wieck and K. Ploog, *Appl. Phys. Lett.* **56**, 928 (1990).
- ⁴T. Bever, A. D. Wieck, K. v. Klitzing, K. Ploog, and P. Wyder, *Phys. Rev. B* (to be published).
- ⁵K. Ismail, D. A. Antoniadis, and H. I. Smith, *Appl. Phys. Lett.* **55**, 589 (1989).
- ⁶A. Palevski, M. Heiblum, C. P. Umbach, C. M. Knoedler, A. N. Broers, and R. H. Koch, *Phys. Rev. Lett.* **62**, 1776 (1989); C. P. Umbach, A. Palevski, M. Heiblum, and U. Sivan, *J. Vac. Sci. Technol. B* **7**, 2003 (1989).
- ⁷S. Y. Chou, D. R. Allee, R. F. W. Pease, and J. S. Harris, Jr., *Appl. Phys. Lett.* **55**, 176 (1989).
- ⁸K.-F. Berggren, T. J. Thornton, D. J. Newson, and M. Pepper, *Phys. Rev. Lett.* **57**, 1769 (1986).
- ⁹G. Timp, A. M. Chang, P. Mankiewich, R. Behringer, J. E. Cunningham, T. Y. Chang, and R. E. Howard, *Phys. Rev. Lett.* **59**, 732 (1987).
- ¹⁰P. H. M. van Loosdrecht, C. W. J. Beenakker, H. van Houten, J. G. Williamson, B. J. van Wees, J. E. Mooij, C. T. Foxon, and J. J. Harris, *Phys. Rev. B* **38**, 10162 (1988).
- ¹¹S. Nakata, Y. Hirayama, S. Tarucha, and Y. Horikoshi, *J. Appl. Phys.* **69**, 3633 (1991).
- ¹²J. K. Jain and S. A. Kivelson, *Phys. Rev. Lett.* **60**, 1542 (1988).
- ¹³A. Sommerfeld and H. Bethe, *Handbuch der Physik von Geiger und Scheel* (Springer, Berlin, 1933).
- ¹⁴A. D. Wieck and K. Ploog, in *Proceedings of the 20th International Conference on Physics of Semiconductors*, edited by E. M. Anastassakis and J. D. Joannopoulos (World Scientific, Singapore, 1990), p. 1697.
- ¹⁵P. Guéret, A. Baratoff, and E. Marclay, *Europhys. Lett.* **3**, 367 (1987).
- ¹⁶H. A. Fertig and B. I. Halperin, *Phys. Rev. B* **36**, 7969 (1987).
- ¹⁷U. Wulf and R. R. Gerhardts, in *Physics and Technology of Submicron Structures*, edited by H. Heinrich, G. Bauer, and F. Kuchar (Springer, Berlin, 1988), p. 162.
- ¹⁸H. van Houten, C. W. J. Beenakker, P. H. M. van Loosdrecht, T. J. Thornton, H. Ahmed, M. Pepper, C. T. Foxon, and J. J. Harris, *Phys. Rev. B* **37**, 8534 (1988).